PHYSICAL REVIEW E **92**, 061001(R) (2015)

Helicity conservation under quantum reconnection of vortex rings

Simone Zuccher*
Department of Computer Science, U. Verona, Ca' Vignal 2, Strada Le Grazie 15, 37134 Verona, Italy

Renzo L. Ricca†
Department of Mathematics & Applications, U. Milano-Bicocca, Via Cozzi 55, 20125 Milano, Italy

(Received 16 April 2015; published 2 December 2015)

Here we show that under quantum reconnection, simulated by using the three-dimensional Gross-Pitaevskii equation, self-helicity of a system of two interacting vortex rings remains conserved. By resolving the fine structure of the vortex cores, we demonstrate that the total length of the vortex system reaches a maximum at the reconnection time, while both writhe helicity and twist helicity remain separately unchanged throughout the process. Self-helicity is computed by two independent methods, and topological information is based on the extraction and analysis of geometric quantities such as writhe, total torsion, and intrinsic twist of the reconnecting vortex rings.

DOI: 10.1103/PhysRevE.92.061001 PACS number(s): 47.32.cf, 67.30.he, 03.75.Lm, 47.37.+q

I. INTRODUCTION

A. Background

Reconnection of coherent structures plays a fundamental role in many areas of science. Examples include vortices in classical fluid flows [1,2], quantum vortex filaments in superfluid helium [3,4], magnetic flux tubes in plasma physics [5,6], phase transitions in mesoscopic physics [7], and macromolecules in DNA biology [8]. Here we focus on a single reconnection event, which characterizes superfluid quantum turbulence [9,10], by analyzing dynamical, geometric, and topological properties that are relevant also in classical viscous fluids [2], where similar features such as time asymmetry [4], helicity transfers, randomization of the velocity field, and energy cascades [11] are important.

In recent months, a number of remarkable results based on experimental observations [12], mathematical analysis [13], and theoretical and numerical work [14] have provided contradictory information regarding helicity transfer through reconnection. On the one hand, laboratory experiments on the production and evolution of vortex knots in water show [12] that the centerline helicity of a vortex filament remains essentially conserved throughout the spontaneous reconnection of the interacting vortices. This result is mirrored by the mathematical analysis of conservation of writhe and total torsion (for definitions, see Sec. III below) under the assumption of antiparallel reconnection of the interacting strands [13]. On the other hand, recent numerical results [14], based on a linearized model of interacting Burgers-type vortices brought together by an ambient irrotational strain field, show that the initial helicity associated with the skewed geometry is eliminated during the process. This apparent contradiction provided further motivation for the present study.

In this paper, we carry out a simulation of the interaction and reconnection of a single pair of identical quantum vortex rings. The evolution is governed by the three-dimensional Gross-Pitaevskii equation (GPE), with the aim to reproduce and analyze in the GPE context the fine details of the prototype reconnection event as studied in [14]. By resolving the fine structure of the vortex cores, we monitor all the relevant dynamical, geometric, and topological features of the reconnection process. Consistently with current simulations (see, for example, [11]), the peak in the normalized total length of the vortex system, given by an initial stretching process followed by its marked decay, is taken as a signature of the reconnection event, providing a precise benchmark for the diagnostics of the mathematical and physical properties associated with the reconnection event.

B. Governing equations

Direct numerical simulation of the reconnecting quantum vortex rings is done by using the 3D GPE,

$$\frac{\partial \psi}{\partial t} = \frac{i}{2}\nabla^2\psi + \frac{i}{2}(1-|\psi|^2)\psi, \tag{1}$$

with background density $\rho_b = 1$. Through the Madelung transformation $\psi = \sqrt{\rho}\exp(i\theta)$, Eq. (1) admits decomposition into two equations that can be interpreted in classical fluid dynamical terms, i.e., the continuity equation and the momentum equation, given by

$$\frac{\partial \rho}{\partial t} + \frac{\partial(\rho u_j)}{\partial x_j} = 0, \tag{2}$$

$$\rho\left(\frac{\partial u_i}{\partial t} + u_j\frac{\partial u_i}{\partial u_j}\right) = -\frac{\partial p}{\partial x_i} + \frac{\partial \tau_{ij}}{\partial x_j}, \tag{3}$$

where $\rho = |\psi|^2$ denotes fluid density, $\boldsymbol{u} = \nabla\theta$ is the velocity, $p = \frac{\rho^2}{4}$ is the pressure, and $\tau_{ij} = \frac{1}{4}\rho\frac{\partial^2 \ln\rho}{\partial x_i \partial x_j}$ denotes the so-called quantum stress ($i,j = 1,2,3$). Defects in the wave function ψ represent infinitesimally thin vortices of constant circulation $\Gamma = \oint \boldsymbol{u}\cdot d\boldsymbol{s} = 2\pi$ of healing length $\xi = 1$. It is well known that the GPE conserves mass, given by $M = \int |\psi|^2\, d\boldsymbol{x}^3$, and the Hamiltonian $E = K + I$, where

$$K = \frac{1}{2}\int \nabla\psi\cdot\nabla\psi^*\, d\boldsymbol{x}^3,\ I = \frac{1}{4}\int (1-|\psi|^2)^2\, d\boldsymbol{x}^3 \tag{4}$$

*simone.zuccher@univr.it
†renzo.ricca@unimib.it

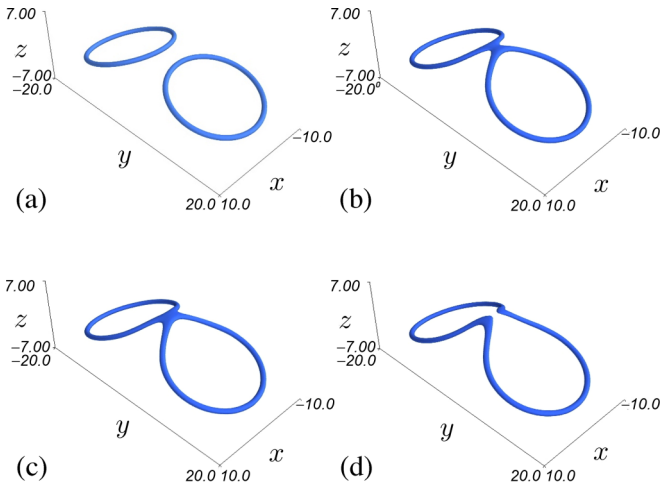

FIG. 1. (Color online) Time-evolution of interaction and reconnection of two quantum vortex rings; isosurfaces of $\rho = 0.06$. (a) $t = 0$, (b) $t = 10$, (c) reconnection time $t = t^* = 11.81$, and (d) $t = 14$.

denote, respectively, the kinetic (K) and interaction (I) energy of the system (ψ^* being the complex conjugate of ψ). The term τ_{ij}, negligible compared to the pressure term at length scales much larger than the healing length $\xi = 1$, is expected to be key to vortex reconnection [4], and at scales larger than the vortex core, the GPE in the form of Eqs. (2) and (3) reduces to the classical compressible Euler equations.

C. Helicity and self-linking number

A fundamental quantity of topological fluid mechanics is kinetic helicity, defined by [15]

$$H = \int \boldsymbol{u} \cdot \boldsymbol{\omega}\, d\boldsymbol{x}^3, \tag{5}$$

where $\boldsymbol{\omega} = \boldsymbol{\nabla} \times \boldsymbol{u}$ is the vorticity, and the integral is extended over the vorticity volume. H is known to be an invariant of ideal fluid flows, and in ideal conditions it admits a topological interpretation in terms of linking number [16]. For a pair of linked vortex rings V_1 and V_2, centered, respectively, on curves C_1 and C_2 and of equal circulation Γ, Eq. (5) can be written as [17,18]

$$H(V_1,V_2) = \Gamma^2[\mathrm{SL}(V_1) + \mathrm{SL}(V_2) + 2\,\mathrm{Lk}(C_1,C_2)], \tag{6}$$

where $H(V_1,V_2)$ is the total helicity of the system, $\mathrm{SL}(V_i)$ is the (Călugăreanu-White) self-linking number of V_k ($k = 1,2$), and $\mathrm{Lk}(C_1,C_2)$ is the (Gauss) linking number of C_1 and C_2. Note that if the pair of rings are unlinked [as in our case, cf. Fig. 1(a)], then $\mathrm{Lk}(C_1,C_2) = 0$, and (6) can be further simplified to

$$H(V_1,V_2) = \Gamma^2[\mathrm{SL}(V_1) + \mathrm{SL}(V_2)]. \tag{7}$$

In general the self-linking number, SL, can be decomposed into global geometric quantities, and one can show [19,20] that $\mathrm{SL}(V_k) = \mathrm{Wr}(C_k) + T(C_k) + N(R_k)$, where the writhing number $\mathrm{Wr}(C_k)$, total torsion $T(C_k)$, and intrinsic twist $N(R_k)$ are quantities that depend solely on the shape of the vortex centerline C_k and ribbon R_k (for definitions, see [13,18] and Sec. III below).

II. NUMERICS AND INITIAL CONDITIONS

The numerical code used for the simulation is described in [4]. It is based on a second-order Strang splitting method in time, and Fourier decomposition in space. Hence, boundary conditions must be periodic; for nonperiodic directions, the computational domain is doubled and "mirror" vortex rings are introduced in the doubled domain, as was done in [21]. The method conserves mass exactly.

Initial conditions

A pair of vortex rings is set at the center of the numerical box. While this particular setting provides a good comparative test for the physics of vortex reconnection [22], it helps to avoid difficulties associated with the numerical implementation of boundary conditions and the topological complexity implied by periodic conditions while offering a realistic match to simulate the event studied in [14].

At time $t = 0$, the two rings are centered in $(0;\pm 10;0)$, have radius $R_0 = 8$, and are mutually inclined by an angle $\alpha = \pm\pi/10$ with respect to the horizontal plane [see Fig. 1(a)]. The computational domain is $[-20;20] \times [-30;30] \times [-20;20]$. To have fine spatial and temporal resolution of the vortex core and of the reconnection process, we have used $\Delta x = \Delta y = \Delta z = \xi/6$ (i.e., the number of points is $240 \times 360 \times 240$) and $\Delta t = 1/80 = 0.0125$.

At each point Q on the vortex ring, we place a Frenet triad $\{\hat{\mathbf{t}},\hat{\mathbf{n}},\hat{\mathbf{b}}\}$ given by the local unit tangent, normal and binormal to the vortex centerline (no inflection points emerge during the simulation). For each grid point P in the numerical domain, we seek the nearest point Q on the vortex line so that $\overrightarrow{QP}$ identifies the distance of P from the vortex. Thus, $\overrightarrow{QP}$ is locally orthogonal to the vortex, in the plane defined by $\hat{\mathbf{n}}$ and $\hat{\mathbf{b}}$ at Q. In this plane, P has polar coordinates (r,θ) centered on Q, where $r = \overline{QP}$ and θ is the angle between $\overrightarrow{QP}$ and $\hat{\mathbf{n}}$.

Each vortex contributes to the initial condition with a density distribution ρ_{0k} given by the Padé approximation [23] $\rho_{0k} = (\frac{11}{32}r^2 + \frac{11}{384}r^4)/(1 + \frac{1}{3}r^2 + \frac{11}{384}r^4)$, and phase distribution θ_{0k}. The initial condition due to the presence of both rings is thus $\psi_0 = \sqrt{\rho_{01}\rho_{02}}\exp[i(\theta_{01} + \theta_{02})]$.

III. EXTRACTION OF GEOMETRIC AND TOPOLOGICAL QUANTITIES

Normalized total length L/ξ, writhe Wr, normalized total torsion T, and intrinsic twist N are the global geometric quantities we want to monitor during reconnection. The total twist is given by $\mathrm{Tw} = T + N$, and together with Wr it gives the self-linking number $\mathrm{SL} = \mathrm{Wr} + \mathrm{Tw}$, a topological invariant. These quantities are well-defined (assuming everything is sufficiently smooth) for each individual vortex ring.

The writhe $\mathrm{Wr} = \mathrm{Wr}(C)$ is analytically defined by

$$\mathrm{Wr} = \frac{1}{4\pi}\int_C\int_C \frac{\mathbf{x}-\mathbf{x}^*}{\|\mathbf{x}-\mathbf{x}^*\|^3}\cdot\left(d\mathbf{x}\times d\mathbf{r}^*\right), \tag{8}$$

where C is the vortex centerline and $\mathbf{x}$ and $\mathbf{x}^*$ denote the position vectors of two points on C.

The normalized total torsion $T = T(C)$ is given by

$$T = \frac{1}{2\pi}\int_C \tau(s)\,ds, \tag{9}$$

where (from its basic definition) the local torsion $\tau(s)$, function of arc-length s on C, involves third-order derivatives of the position vector $\mathbf{x}$ of any point on C.

Intrinsic twist $N = N(R)$ measures the rotation around C of a reference ribbon R (with baseline C) as we move along C. Here R has edges given by C and C', a second curve obtained by translating C a small distance ϵ (the width of R) along a unit normal vector $\hat{\mathbf{u}}$ to C. ϵ is chosen to be constant along C and sufficiently small compared to the local radius of curvature. Clearly R depends on the choice of $\hat{\mathbf{u}}$, and in the absence of inflection points this is always well-defined [17,18]. If $\varphi(s)$ denotes the angle between $\hat{\mathbf{u}}$ and $\hat{\mathbf{n}}$, we have

$$N = \frac{1}{2\pi}\int_C \frac{d\varphi(s)}{ds}\,ds = \frac{[\Phi]_C}{2\pi}, \tag{10}$$

which measures the number of full rotations of the ribbon R after one full turn along C. From the definition of total twist, one can show [18] that indeed $\mathrm{Tw} = T + N$.

IV. RESULTS

Vortex centerlines are extracted from numerical data, first by isolating the tubes whose density $\rho < 0.2$, and then by looking for minima of $\rho/|\boldsymbol{\omega}|$ (minima of density correspond to maxima of vorticity). Particular care has been taken to extract sufficiently smooth data. Intrinsic twist is obtained from phase information. The ribbon R is thus obtained by requiring constant phase $\theta = \bar{\theta}$ along C, and by setting $\epsilon = 0.3$, a good compromise is reached between visualization needs and misleading effects. As usual, smoothing was applied to ensure sufficient regularity.

Figure 1 shows four snapshots of the time evolution of interaction and reconnection of the quantum vortex rings (isosurfaces of $\rho = 0.06$). Before reconnection, the two vortex rings move toward each other, bending upward in the region near the reconnection site, with the more distant parts of the vortices remaining almost unaffected. The change of normalized total length L/ξ of the pair of rings against time is used to check the reconnection process and to detect the reconnection time. The plot is shown in Fig. 2 for $t \in (10,14)$. The marked peak at $t = t^* = 11.81$, after stretching, is taken as a signature of the reconnection time. The maximum value $L_{\max} \approx 108.6\,\xi$ corresponds to about 8% of an increase with respect to the initial total length, given by $L_0 \approx 100.5\,\xi$. For $t > t^*$, the system relaxes at a faster rate, confirming the time asymmetry found in earlier work [4].

As a further check, we plot the Hamiltonian (E) given by the normalized total energy $(K + I)/E$ and, separately, the normalized kinetic energy K/E and interaction energy I/E, given by (4) [see Fig. 3(a)]. Kinetic helicity is computed according to Eq. (5). As shown in Fig. 3(b), its value remains bounded, i.e., $|H| < 10^{-9}$, which is approximately zero throughout the reconnection process [at these length scales, the spikes of the plot in Fig. 3(b) are essentially due to numerical noise]. A check on vortex strength confirms the conservation of Γ before and after reconnection. A closeup view of the vortex centerlines (in red) and reference ribbons (green and blue) immediately before and after reconnection is shown in the plots of Figs. 4(a) and 4(b). The reconnection event takes place at a much faster time scale, well beyond numerical accuracy. To monitor as closely as possible the topological transition, the event is represented at maximum numerical resolution by showing the diagrams of the discretized vortex centerlines in Fig. 5(c). As we can see from the central diagram of Fig. 5(c) (at $t = t^*$), the reconnecting event is numerically triggered by a jump at the two nodal points (circles) of closest approach, demonstrating that in the limit of numerical resolution, reconnection involves only the mutual cancellation of two antiparallel polygonal segments.

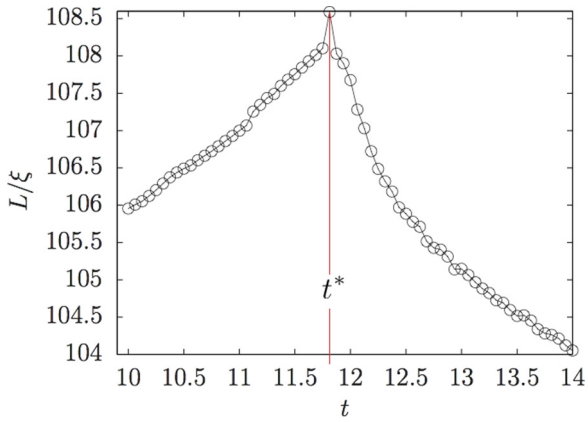

FIG. 2. (Color online) Normalized total length L/ξ, plotted against time t. The peak in L/ξ is taken as signature of the reconnection time at $t = t^* = 11.81$.

Finally, we examine the individual contributions to the self-linking number by using the independent equations (8)–(10). Plots of Wr, T, N, and SL against time are shown in Fig. 5. The ribbon R is found to be $\theta = \bar{\theta} \approx 50^\circ$. Writhe and twist remain very small throughout the process. They are identically zero only at $t = 0$ when the vortex rings are exactly planar tori, whereas for $t > 0$ the vortex centerlines become gradually deformed. Except for a few spikes, which are not related to reconnection, $|\mathrm{Wr}| < 10^{-4}$ and $|\mathrm{Tw}| < 2 \times 10^{-4}$. Numerical errors associated with the computation of Tw are generally larger than those on Wr because of the higher-order derivatives involved in the computation of the normalized total torsion [see Fig. 5(b)] and the additional numerical noise associated

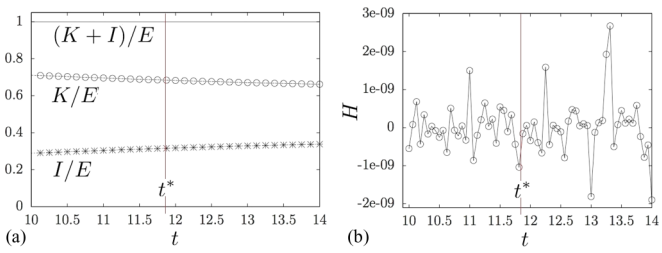

FIG. 3. (Color online) (a) Normalized total energy (Hamiltonian) $(K + I)/E$, normalized kinetic energy K/E, and normalized interaction energy I/E plotted against time t. (b) Kinetic helicity H plotted against time t. The vertical (red) line denotes the reconnection time $t = t^* = 11.81$.

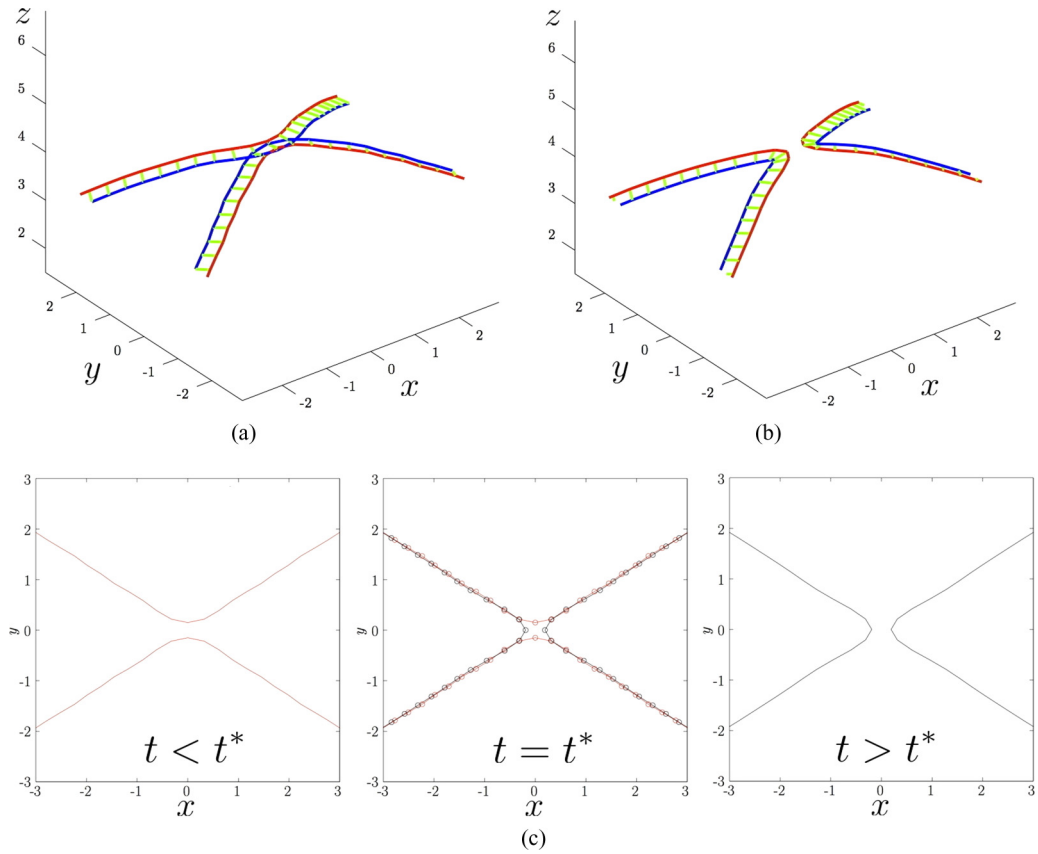

FIG. 4. (Color online) A closeup view of the vortex centerlines (red) and reference ribbons (green and blue, pale gray, and darker otherwise) (a) immediately before reconnection at $t = 11.81$ and (b) immediately after reconnection at $t = 11.88$. The transition is shown at maximum numerical resolution: (c) vortex centerlines just before ($t < t^*$, red) and after ($t > t^*$, black) reconnection; the state in-between (at $t = t^*$) shows that reconnection is numerically triggered by a jump at just two nodal points (circles).

with the computation of N [see Fig. 5(c)]. The numerical code has been validated by computing Wr and Tw of known benchmarks, and we are confident that the reported spikes are only due to an accumulation of numerical errors. Thus, we conclude that all plots of Fig. 5 show consistently $\mathrm{Wr} = T = N = \mathrm{SL} = 0$ throughout the reconnection process.

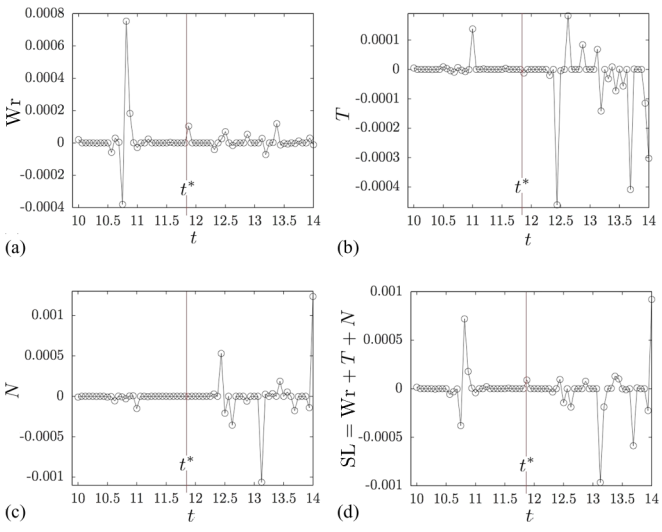

FIG. 5. (Color online) (a) Writhe (Wr), (b) normalized total torsion (T), (c) normalized intrinsic twist (N) (with $\bar{\theta} \approx 50^\circ$), and (d) self-linking number (SL) plotted against time t. The vertical line (red) denotes the reconnection time $t = t^* = 11.81$.

V. CONCLUSIONS

We have performed numerical simulations of the GPE that resolve the fine structure of the vortex core under antiparallel reconnection of the tube strands of two colliding quantum vortex rings. This simple scenario provides a good benchmark for comparison with earlier works on direct numerical simulation of reconnecting vortex rings under Navier-Stokes equations [24,25], and an ideal setup for clarifying recent contradictory results obtained by experiments and theoretical modeling on classical vortex dynamics.

Reconnection under Gross-Pitaevskii is clearly manifested by the generation of a peak in total length, and this is taken as a marker of the reconnection event. We took extra care to monitor the behavior of several geometric quantities during reconnection. As predicted by geometric analysis [13], writhe and total torsion are found to remain conserved, whereas there is no change in total intrinsic twist, all these clearly maintaining the self-linking number invariant. Self-helicity, computed independently by using Eq. (5), is found consistently to remain conserved during reconnection. Since in our experiment the (Gauss) linking number Lk is always

zero (the rings remain unlinked throughout the process), there is no contradiction with the fact that during reconnection topology actually changes (as indeed happens here). The fact that self-helicity, and hence total helicity, remains conserved during reconnection is thus something not only new for quantum systems, but also in good agreement with the recent experimental observations of reconnecting vortices in water [12]. The methods used here can certainly be extended to study more complex topologies, and further work is indeed underway to analyze and to extend these preliminary findings.

[1] S. Kida and M. Takaoka, Annu. Rev. Fluid Mech. **26**, 169 (1994).
[2] A. K. M. F. Hussain and K. Duraisamy, Phys. Fluids **23**, 021701 (2011).
[3] M. S. Paoletti, M. E. Fisher, and D. P. Lathrop, Physica D **239**, 1367 (2010).
[4] S. Zuccher, M. Caliari, A. W. Baggaley, and C. F. Barenghi, Phys. Fluids **24**, 125108 (2012).
[5] Y. T. Lau and J. M. Finn, Phys. Plasmas **3**, 3983 (1996).
[6] E. Priest and T. Forbes, *Magnetic Reconnection* (Cambridge University Press, Cambridge, 2000).
[7] S. Lugomer, J. Fluids Struct. **13**, 647 (1999).
[8] A. V. Vologodskii, N. J. Crisona, B. Laurie, P. Pieranski, V. Katritch, J. Dubochet, and A. Stasiak, J. Mol. Biol. **278**, 1 (1998).
[9] W. F. Vinen, Philos. Trans. R. Soc. London, Ser. A **366**, 2925 (2008).
[10] C. F. Barenghi, L. Skrbek, and K. R. Sreenivasan, Proc. Natl. Acad. Sci. (USA) **111**, 4647 (2014).
[11] R. M. Kerr, Phys. Rev. Lett. **106**, 224501 (2011).
[12] M. W. Scheeler, D. Kleckner, D. Proment, G. L. Kindlmann, and W. T. M. Irvine, Proc. Natl. Acad. Sci. (USA) **111**, 15350 (2014).
[13] C. E. Laing, R. L. Ricca, and De. W. L. Sumners, Sci. Rep. **5**, 9224 (2015).
[14] Y. Kimura and H. K. Moffatt, J. Fluid Mech. **751**, 329 (2014).
[15] P. G. Saffman, *Vortex Dynamics* (Cambridge University Press, Cambridge, 1992).
[16] H. K. Moffatt, J. Fluid Mech. **35**, 117 (1969).
[17] R. L. Ricca and H. K. Moffatt, in *Topological Aspects of the Dynamics of Fluids and Plasmas*, edited by H. K. Moffatt *et al.* (Kluwer, Dordrecht, 1992), p. 225.
[18] H. K. Moffatt and R. L. Ricca, Proc. R. Soc. London, Ser. A **439**, 411 (1992).
[19] G. Călugareănu, Chechoslovak Math. J. **11**, 588 (1961).
[20] J. H. White, Am. J. Math. **91**, 693 (1969).
[21] J. Koplik and H. Levine, Phys. Rev. Lett. **71**, 1375 (1993).
[22] P. M. Walmsley, P. A. Tompsett, D. E. Zmeev, and A. I. Golov, Phys. Rev. Lett. **113**, 125302 (2014).
[23] N. G. Berloff, J. Phys. A **37**, 1617 (2004).
[24] S. Kida, M. Takaoka, and F. Hussain, Phys. Fluids A **1**, 630 (1989).
[25] P. Chatelain, D. Kivotides, and A. Leonard, Phys. Rev. Lett. **90**, 054501 (2003).